UC Davis

UC Davis Previously Published Works

Title

Prevention of Collagen-Induced Platelet Binding and Activation by Thermosensitive Nanoparticles

Permalink

https://escholarship.org/uc/item/9586s64h

Journal

The AAPS Journal, 17(5)

ISSN

1550-7416

Authors

McMasters, James
Panitch, Alyssa

Publication Date

2015-09-01

DOI

10.1208/s12248-015-9794-9

Peer reviewed

eScholarship.org Powered by the California Digital Library
University of California

The AAPS Journal, Vol. 17, No. 5, September 2015 (© 2015)
DOI: 10.1208/s12248-015-9794-9

Research Article

Theme: Clinical and Commercial Translation of Drug Delivery Systems
Guest Editors: Yoon Yeo and Craig Svensson

Prevention of Collagen-Induced Platelet Binding and Activation by Thermosensitive Nanoparticles

James McMasters[1] and Alyssa Panitch[1,2]

Received 24 February 2015; accepted 30 May 2015; published online 13 June 2015

ABSTRACT. Peripheral artery disease is an atherosclerotic occlusion in the peripheral vasculature that is typically treated via percutaneous transluminal angioplasty. Unfortunately, deployment of the angioplasty balloon damages the endothelial layer, exposing the underlying collagen and allowing for the binding and activation of circulating platelets, which initiate an inflammatory cascade leading to eventual restenosis. Here, we report on the development of poly(NIPAm-MBA-AMPS-AAc) nanoparticles that have a collagen I-binding peptide crosslinked to their surface allowing them to bind to exposed collagen. Once bound, these particles mask the exposed collagen from circulating platelets, effectively reducing collagen-mediated platelet activation. Using collagen I-coated plates, we demonstrate that these particles are able to bind to collagen at concentrations above 0.5 mg/mL. Once bound, these particles inhibit collagen-mediated platelet activation by over 60%. Using light scattering and zeta potential measurements, we investigated the potential of the nanoparticles as a drug delivery platform. We have verified that the collagen-binding nanoparticles retain the temperature sensitivity common to poly(NIPAm)-based nanoparticles while remaining colloidally stable in aqueous environments. We also demonstrate that they are able to passively load and release anti-inflammatory cell penetrating peptides. Combined, we have developed a collagen-binding nanoparticle that has dual therapy potential, preventing collagen-mediated platelet activation while delivering water-soluble therapeutics directly to the damaged area.

KEY WORDS: collagen; nanoparticle; platelet activation; poly(NIPAm); thermosensitive.

INTRODUCTION

Peripheral artery disease (PAD) is an atherosclerotic occlusive disease that occurs within the peripheral limb arteries. Despite increased awareness and advances in treatment and prevention, 25% of adults over the age of 55 develop PAD, and this incidence rate increases with age and other cardiovascular risk factors such as smoking and hypertension (1–6). PAD is also associated with increased cardiovascular morbidity, such that the development of an effective long-term treatment is important for the large population affected by this disease (7,8).

The current standard of surgical treatment for severe PAD is percutaneous transluminal angioplasty, with the possible deployment of a stent to hold open the widened vessel. Unfortunately, deployment of the balloon during the angioplasty procedure damages the vessel wall, stripping off the endothelial cells of the internal lumen and exposing the underlying collagenous tissue (9). Platelets in the circulating blood are able to bind to the exposed collagen and become activated (10,11), releasing multiple proinflammatory factors such as epidermal growth factor, and platelet derived growth factor, which can lead to the activation of smooth muscle cells (SMC), resulting in SMC proliferation and intimal hyperplasia (12–16). Additionally, the activated SMC release multiple proinflammatory factors such as interleukin-1β (IL-1β), interleukin-6 (IL-6), and tumor necrosis factor-α (TNF-α), which serve to perpetuate the inflammatory cascade, resulting in continued SMC proliferation, extracellular matrix (ECM) synthesis, and eventual restenosis of the treated vessel (12,17).

This restenosis is prevented, when possible, using drug-eluting stents that can release cytostatic compounds such as paclitaxel or sirolimus, which have been shown to effectively inhibit SMC proliferation (18–20). However, these compounds are non-targeted and thus also affect the local endothelial cells as well as the proliferating SMCs. This inhibits endothelial migration and proliferation (19,20), preventing reendothelialization of the damaged vessel and leaving the collagen and the drug-eluting stent chronically exposed to the circulating blood, which can lead to complications such as late stent thrombosis (21,22). Additionally, stents deployed to treat PAD show fracture rates as high as

[1] Weldon School of Biomedical Engineering, Purdue University, 206 S. Martin Jischke Dr., West Lafayette, Indiana 47907, USA.
[2] To whom correspondence should be addressed. (e-mail: apanitch@purdue.edu)

 1550-7416/15/0500-1117/0 © 2015 American Association of Pharmaceutical Scientists

50% due to the higher torsional and crushing forces experienced in the peripheral vasculature (23–25). Together, these problems make stent deployment a sub-optimal solution for the treatment of PAD, as it prevents proper healing of the damaged vessel, while carrying the risk of fracture and all of its associated complications. Therefore, a need exists for a treatment system that can prevent the initial inflammatory response and subsequent SMC activation and proliferation while allowing for endothelial proliferation and eventual healing of the damaged vessel.

Poly(N-isopropylacrylamide) (poly(NIPAm)) is a thermosensitive polymer that has been extensively studied for use in biomedical applications such as tissue engineering, drug delivery, and injectable hydrogels (26–29), as it exhibits a physiologically relevant lower volume phase transition temperature (VPTT) around 33°C (30–33). This temperature sensitivity makes crosslinked poly(NIPAm) nanoparticles ideal *in vivo* drug carriers as they are soluble in aqueous solutions at temperatures below the VPTT, allowing for efficient loading of water-soluble therapeutics via passive diffusion (31,34). The nanoparticles then undergo hydrophobic phase separation at physiological temperatures. Depending on the application, this collapse can trigger rapid burst release of the loaded drug or can result in decreased porosity and a more controlled drug release profile (35–37). Additionally, poly(NIPAm) is readily copolymerized with acrylic acid (AAc), which adds easily modified carboxylic acid functional groups to the backbone of the particle, allowing for the addition of targeting ligands while simultaneously increasing the colloidal stability of the nanoparticle (38–42). In addition to carboxylic acid, the charged sulfated comonomer 2-acrylamido-2-methyl-1-propanesulfonic acid (AMPS) has been added to poly(NIPAm) nanoparticles, resulting in colloidally stable, hemocompatible sulfated poly(NIPAm-AMPS) nanoparticles (29,43,44).

Our lab has previously developed a mimic of the proteoglycan decorin named DS-SILY, which consists of a collagen I-binding peptide attached to a dermatan sulfate backbone (45,46). DS-SILY has been shown to specifically bind to type I collagen, prevent platelet adhesion and activation, and promote endothelial migration on a collagen-coated surface (46). The collagen-binding properties of DS-SILY are mainly attributed to the collagen I-binding peptide sequence, while the platelet binding inhibition is attributed to competition from the SILY peptide as well as to the dermatan sulfate backbone, which serves as a hydrophilic barrier to further prevent platelet attachment. When modified with the SILY peptide, poly(NIPAm) nanoparticles can bind to exposed collagen to provide a similar hydrophilic barrier, and when delivered directly to the damaged vessel via porous catheter balloon, or through the end of a standard catheter, we expect that they can prevent platelet adhesion and activation while allowing for the release of therapeutics that have been loaded into the nanoparticle core. We have developed a family of anti-inflammatory cell-penetrating peptides that have been shown to inhibit mitogen activated protein kinase activated protein kinase 2 (MK2). One of these peptides, KAFAKLAARLYRKALARQLGVAA (KAFAK), has been shown to reduce the expression of proinflammatory cytokines such as IL-6 and TNF-α in doses as low as 10 μM (47). KAFAK's potency, combined with its cationic charge, makes it an ideal candidate for loading into anionic drug delivery systems such as our sulfated nanoparticles. Here, we apply this information to show that a sulfated poly(NIPAm)-based nanoparticle drug delivery system modified with a collagen I-binding peptide is able to bind specifically to a collagen-coated surface and prevent platelet activation in a manner similar to DS-SILY, while retaining their ability to load and release water-soluble therapeutics such as KAFAK. In addition to the particles' platelet inhibition and drug release capabilities, we also investigate their collagen binding affinity, as well as the effects of the addition of the collagen-binding peptide on the particles' size, temperature sensitivity, and surface charge.

MATERIALS AND METHODS

Nanoparticle Synthesis

NIPAm-based nanoparticles, with 5% AMPS and 1% AAc were synthesized using a standard precipitation polymerization reaction (48). First, 39 mL of MilliQ water (18.2 MΩ·cm resistivity, Millipore) was heated to 70°C in a 3-neck round bottom flask and refluxed under nitrogen for 30 min; 794.1 mg of NIPAm (Thermo Fisher Scientific), 28.5 mg of N,N′-methylenebisacrylamide (MBA, Sigma-Aldrich), and 76.5 mg of AMPS (Sigma-Aldrich) were dissolved in 10 mL of MilliQ water and then added to the flask. Five microliters of AAc (99.5%, Thermo Fisher Scientific) and 164 μL of sodium dodecyl sulfate (SDS, 10% *w/v*, Sigma-Aldrich) were added, and the solution was allowed to mix for 5 min. Finally, 33.7 mg of potassium persulfate (Sigma-Aldrich) was dissolved in 1 mL of MilliQ water and added to the flask to initiate the polymerization reaction. The reaction was allowed to proceed for 5 h, with water levels being adjusted to maintain the initial 50-mL reaction volume. After 5 h, the reaction was cooled to room temperature and then dialyzed against MilliQ water for 7 days using a 15,000 MWCO dialysis membrane (Spectra-Por). Following dialysis, the purified poly(NIPAm-MBA-AMPS-AAc) nanoparticles were lyophilized and stored at room temperature.

Peptide Attachment

Collagen-binding nanoparticles were fabricated by using 1-ethyl-3-(3-dimethylaminopropyl)carbodiimide hydrochloride (EDC) to react the free carboxyl groups present on the nanoparticles with the hydrazide of the heterobifunctional cross linker N-β-Maleimidopropionic acid hydrazide (BMPH). The maleimide group of BMPH was then reacted with the free thiol group on the C-terminal cysteine of the collagen-binding peptide, resulting in a peptide-conjugated nanoparticle. First, lyophilized poly(NIPAm-MBA-AMPS-AAc) nanoparticles were dissolved at 1.0 mg/mL in coupling buffer consisting of 0.1 M MES (Sigma-Aldrich), 0.5 M NaCl (Sigma-Aldrich) at pH 6.0. EDC (0.4 mg/mL; Thermo Fisher Scientific) and the solution was allowed to shake at room temperature for 15 min. For 100% peptide-modified particles, a 1:1 molar equivalent of BMPH (BMPH/AAc) was then added to the solution and allowed to shake at room temperature for 30 min. Finally, the BMPH-conjugated

nanoparticles were purified by size exclusion chromatography on an AKTA purifier FPLC (GE Healthcare) and lyophilized.

The lyophilized NP-BMPH were dissolved at 1 mg/mL in 1× PBS, and 1% of the total concentration of the collagen-binding peptide RRANAALKAGELYKSILYGC (SILY, 80% purity, Genscript) was added as $SILY_{biotin}$ and allowed to shake at room temperature for 45 min. The remaining peptide was then added and allowed to react for an additional 90 min, to create the SILY-modified nanoparticles (NP-SILY). Non-collagen-binding particles were made by following the same protocol and adding the peptide GVDVDQDGETGC (LFA, 78% purity, Genscript) instead of SILY, to create LFA-modified particles (NP-LFA). For 100% modified nanoparticles, a 1 molar excess (as compared to total estimated BMPH content) of SILY was added to ensure complete attachment to the BMPH. The final compositions of the modified nanoparticles are summarized in Table I. The modified particles were then purified by size exclusion chromatography, lyophilized, and stored at room temperature.

Peptide Attachment Assay

Covalent attachment of the peptide to the nanoparticle was verified with a streptavidin-HRP colorimetric assay (R&D Systems). Nanoparticles were dissolved at 1 mg/mL in diluted streptavidin solution and allowed to shake on a vortex shaker for 20 min. The particles were pelleted via centrifugation at 18,000×*g* for 20 min and rinsed three times with 1× PBS before being resuspended at 1 mg/mL in a reagent color solution consisting of a 1:1 mixture of hydrogen peroxide and tetramethylbenzidine, and allowed to shake on a vortex shaker for 20 min. Finally, 2N H_2SO_4 was added to stop the reaction, and the absorbance was read at 450 and 540 nm on a SpectraMax M5 plate reader (Molecular Devices). Particles fabricated using the above method but without the BMPH crosslinker were also tested to verify covalent, rather than electrostatic, attachment of the SILY to the nanoparticle surface.

Nanoparticle Characterization

The hydrodynamic radius of all particles was measured using dynamic light scattering (DLS) on a Nano-ZS90 Zetasizer (Malvern). Nanoparticles were dissolved at 0.1 mg/mL in MilliQ water in a disposable polystyrene cuvette and were subjected to a minimum of 12 runs at 25 and 37°C after equilibrating at the desired temperature for 5 min. Five runs were completed for each batch of particles, and three sets of particles were synthesized and tested to demonstrate reproducibility of the synthesis. Zeta potentials and electrophoretic mobility were obtained on a Nano-ZS90 Zetasizer at the same sample concentration in MilliQ water using folded capillary cells, with the mobility data being obtained from five runs of a single set of particles.

Table I. SILY Molar Reaction Ratios

Name	Peptide/BMPH molar ratio
100% NP-SILY	2:1
50% NP-SILY	0.5:1
25% NP-SILY	0.25:1
0% NP-SILY	0:1
NP-LFA	2:1

Peptide Loading and Release

To determine the ability of the modified nanoparticles to load and release cationic therapeutics, we loaded the nanoparticles with the anti-inflammatory cell-penetrating peptide KAFAK (American Peptide). To load the nanoparticles, 100% SILY-modified nanoparticles and KAFAK were co-incubated in MilliQ water at final concentrations of 1 and 2 mg/mL, respectively, and stored at 4°C for 24 h. Loaded nanoparticles were pelleted via centrifugation, and the supernatant was collected for analysis. To measure peptide release, the loaded nanoparticles were resuspended in 37°C PBS and 75 μL aliquots were taken at predetermined intervals. The nanoparticles were pelleted via centrifugation and the supernatant was collected. A fluoraldehyde o-phthalaldehyde (OPA) assay was performed to determine the amount of KAFAK loaded into and released by the modified nanoparticles. Briefly, 1:10 mixtures of sample and fluoraldehyde OPA were created in opaque 96-well plates (VWR), and the fluorescence was measured at an excitation of 360 nm and emission of 455 nm on a SpectraMax M5 plate reader. Values were compared against a standard to determine the amount of KAFAK present in each solution.

Collagen Binding Affinity

The collagen binding affinity of the modified nanoparticles was tested using a streptavidin-HRP colorimetric assay to detect the presence of the biotinylated particles on a collagen-coated surface. Collagen-coated 96-well plates (Corning Biocoat, VWR) were blocked with 1% bovine serum albumin (BSA, VWR) in 1× PBS for 1 h at room temperature. The blocking solution was removed, and modified nanoparticles dissolved in 1% BSA in 1× PBS at concentrations between 0 and 8 mg/mL were added to the plate and incubated on a plate shaker at 37°C and 200 RPM for 30 min. The plate was rinsed three times with 1× PBS and 100 μL of a diluted streptavidin-HRP solution was added to each well and allowed to incubate on a plate shaker at room temperature and 200 RPM for 20 min. The plate was again rinsed three times with 1× PBS and 100 μL of reagent color solution was added to each well and allowed to incubate on a plate shaker at room temperature and 200 RPM for 20 min. Finally, 50 μL of 2N H_2SO_4 was added to stop the reaction, and the absorbance was read at 450 and 540 nm on a SpectraMax M5 plate reader.

Platelet Inhibition

The ability of modified nanoparticles to inhibit platelet activation was determined by dissolving modified nanoparticles in 1× PBS and incubating 50 μL aliquots on a collagen coated plate at 37°C and 200 RPM for 30 min. Fifteen milliliters of whole blood was collected into citrated vacutainers from healthy volunteers by venipuncture following an approved Purdue IRB protocol and with informed consent. The blood was centrifuged for 20 min at 200×*g* and

25°C, and the top layer of platelet-rich plasma (PRP) was collected. The plates were rinsed three times with 1× PBS and 50 μL of PRP was added to each well and allowed to incubate at room temperature for 1 h. Following the incubation, 45 μL was removed from each well and mixed with 5 μL ETP (107 mM EDTA, 12 mM theophylline, and 2.8 mM prostaglandin E_1) to stop further platelet activation (46). The platelets were pelleted via centrifugation and the supernatant was diluted 1:10,000 in 1% BSA in 1× PBS and then run on a sandwich ELISA for platelet factor 4 (PF-4) and β-thromboglobulin (NAP-2) (R&D Systems) according to the manufacturer protocol.

RESULTS

Effect of Peptide Attachment on Nanoparticle Size and Charge

Due to the importance of NIPAM's temperature sensitivity, we investigated how the conjugation of collagen-binding peptides to the surface of the nanoparticles affected their ability to undergo temperature-induced size changes. The effect of peptide conjugation on the hydrodynamic radius of the nanoparticles is shown in Fig. 1. As expected for NIPAm-based particles, we observed a decrease in hydrodynamic radius at temperatures above the VPTT, with the radius decreasing 14.3% when the particle collapsed at temperatures above the VPTT. Addition of the SILY peptide served to reduce the magnitude of the collapse to between 9.3 and 13.2%. The data in Figs. 1 and 2a represent triplicates of SILY-modified nanoparticles with error bars representing the standard deviation, while the data in 2b is from a single batch of SILY-modified nanoparticles run in triplicate.

The zeta potentials and electrophoretic mobility of the particles were investigated to gain insight into the particles surface charge and expected colloidal stability (43,49). Additionally, the change in charge after peptide conjugation provided insight into whether peptides were successfully attached, as the positively charged SILY peptide neutralizes some of the surface charge when covalently bound to the surface of the oppositely charged particle with an increase in the overall potential (less negative) and lower mobility following the addition of the SILY peptide (Fig. 2). Additionally, the zeta potentials of the particles remained unchanged above the VPTT, while particle mobility increased at the higher temperature. This consistency can be attributed to the fact that the overall surface charge density would remain constant due to polymer rearrangement during collapse.

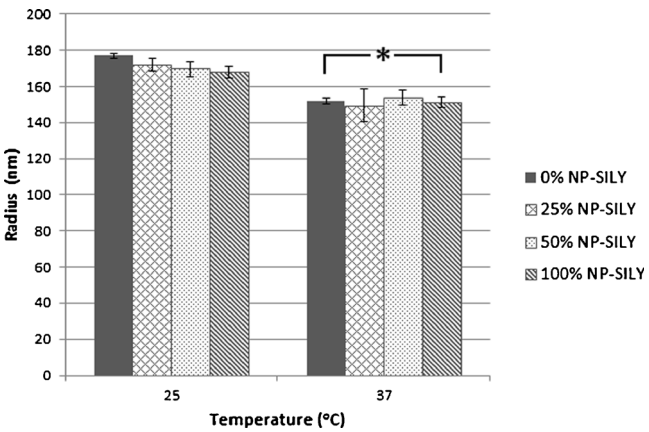

Fig. 1. DLS measurements of the hydrodynamic radius of nanoparticles at 25 and 37°C. The addition of SILY to the surface of the particles reduced the magnitude of the hydrophobic collapse. *Asterisk* indicates statistically significant collapse of particle size at 37°C compared to its respective size at 25°C

Peptide Attachment Assay

To validate that the peptide was covalently crosslinked to the particle and not just physically adsorbed, the presence of biotinylated SILY on the surface of the nanoparticles synthesized with and without BMPH was detected by absorbance reading from a streptavidin-HRP colorimetric assay (Table II). The increase in absorbance on the SILY-modified nanoparticles indicates the presence of $SILY_{biotin}$ on the surface of the nanoparticles. As seen in Table II, particles with BMPH-crosslinked SILY exhibited a 15-fold increase in absorbance compared to those without BMPH, indicating while there is some amount of electrostatic association between the peptide and the nanoparticle; the majority of the SILY is covalently bound to the particles and not simply electrostatically associated.

Peptide Loading and Release

Loading and release of the anti-inflammatory peptide KAFAK from the modified nanoparticles was measured with a fluoraldehyde OPA assay. When coincubated for 24 h at 4°C, the nanoparticles successfully loaded 0.47 mg of KAFA FK, giving them a final loading efficiency (as a percent of final particle weight) of 32%. The loaded nanoparticles demonstrated the ability to release the loaded KAFAK over a period of 24 h, with 78% of the total release occurring in the first 12 h (Fig. 3). Despite the rapid initial release rate, over 70% of the loaded KAFAK remained in the nanoparticles after 120 h, suggesting that it may be permanently associated with the nanoparticle.

Collagen Binding Affinity Assay

The ability of SILY-modified nanoparticles to bind to a collagen-coated surface was confirmed through the use of a streptavidin-HRP colorimetric assay. The binding of the modified particles to collagen is the first step in the inhibition of collagen-mediated platelet activation. As seen in Fig. 4, the particles successfully demonstrated an ability to bind to type I collagen.

When measured against the LFA (A non-collagen-binding peptide)-modified particles, The SILY-modified particles were able to bind to collagen, with the 25% NP-SILY demonstrating attachment at concentrations above 4 mg/mL. Increasing the amount of SILY attached to the particle results in a corresponding increase in collagen binding, with the 50% NP-SILY binding at 2 mg/mL, and the 100% NP-SILY binding at a concentration of 0.25 mg/mL. The NP-LFA particles, modified with a non-collagen-binding peptide, showed no binding to the collagen plate at concentrations up to 8 mg/mL. This indicates that the binding curves shown

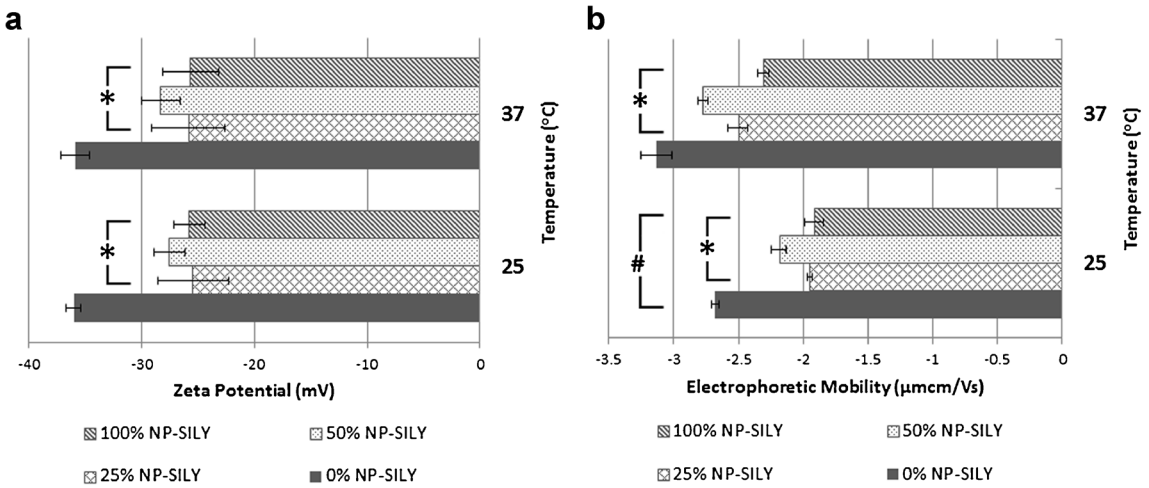

Fig. 2. Zeta potential and electrophoretic mobility measurements of the modified particles show an increase in net charge following the addition of SILY, while surface charge remained unchanged at temperatures above the VPTT (**a**). Particle mobility was reduced following SILY addition, but increased at temperatures above the VPTT (**b**). *Asterisk* indicates significance from corresponding unmodified particle. *Number sign* indicates significance from corresponding particle at 37°C

with the NP-SILY particles are a result of the SILY peptide actively binding to the collagen, as opposed to nonspecific binding of the particles to the surface.

Inhibition of Platelet Activation

The inhibition of collagen-induced platelet activation was measured by the release of PF-4 and NAP-2, two known factors released by activated platelets (50,51). As seen in Fig. 5, platelet activation was inhibited with increasing concentrations of NP-SILY, with maximum inhibition observed at 2 mg/mL, resulting in a greater than 60% inhibition of both PF-4 and NAP-2.

Because the collagen binding assay showed similar levels of binding for the 50 and 25% NP-SILY, only the 50% NP-SILY was tested for effectiveness of platelet inhibition. The 50% SILY-modified nanoparticles showed greater inhibition of PF4 than their 100% SILY-modified counterparts at 0.5 and 1 mg/mL. This increased inhibition disappeared at particle concentrations above 1 mg/mL. At higher concentrations, both the 100% NP-SILY and 50% NP-SILY demonstrated similar levels of platelet inhibition, indicating that there may be a minimum level of NP-SILY binding that is necessary to prevent platelet attachment and activation. Once this minimum binding level is achieved, the nanoparticle coating on the collagen is dense enough to effectively prevent platelet activation, resulting in no further increases with increased nanoparticle concentration.

Table II. $SILY_{biotin}$ Crosslinking to Nanoparticles

Sample name	Absorbance (mAu)
Nanoparticle	0.02±0.003
Nanoparticle-SILY (no BMPH)	0.10±0.001[a]
Nanoparticle-BMPH-SILY	1.52±0.004[a, b]

Results of streptavidin-HRP assay indicate SILY is covalently crosslinked to the nanoparticles via BMPH
[a] Significance from bare nanoparticles
[b] Significance from non-crosslinked nanoparticle-SILY

DISCUSSION

Platelet adhesion and activation on collagen exposed by deployment of an angioplasty balloon releases proinflammatory factors that result in SMC activation and migration, and eventual restenosis (9,12–15). Here, we demonstrate that a sulfated collagen-binding poly(NIPAm-MBA-AMPS-AAc) nanoparticle is able to competitively bind to exposed collagen and prevent collagen-mediated platelet binding and activation while retaining its ability to load and release anti-inflammatory cell-penetrating peptides.

Because the temperature sensitivity is such a crucial characteristic of poly(NIPAm)-based nanoparticle drug delivery systems, retention of this ability following attachment of SILY is critical for the particles to remain an attractive drug delivery platform. Previous studies have shown that the addition of hydrophilic co-monomers to poly(NIPAm) results in decreased temperature sensitivity of the resulting nanoparticles as the charged groups serve to increase overall solubility and resist the temperature-induced hydrophobic collapse (39,52,53). The addition of multiple hydrophilic groups to the backbone of our particles presents a possibility that their temperature sensitivity could be reduced to the extent that they are no longer a viable mechanism of controlled drug loading and release. Previous work on similar sulfated poly(NIPAm-MBA-AMPS) nanoparticles showed a 20% decrease in particle diameter at temperatures above the VPTT. These particles were able to serve as a controlled release platform for therapeutic peptides, with release being observed for up to 1 week *in vitro* (43,44). Our unmodified particles demonstrated similar size change of 14.3%, with the smaller size change being attributed to the addition of the hydrophilic AAc to the polymer chain. Addition of the SILY peptide to the surface initially serves to further resist the particles' hydrophobic collapse, though no further changes are observed with increased SILY addition (Fig. 1).

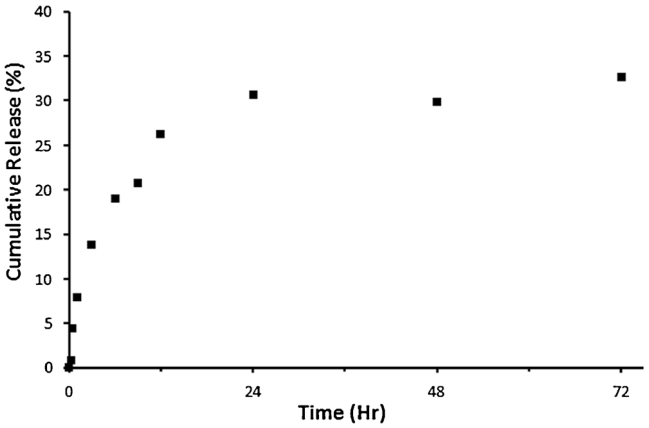

Fig. 3. Results of a fluoraldehyde OPA assay to quantify KAFAK release from the 100% SILY-modified nanoparticles. SILY-modified nanoparticles exhibited an initial burst release followed by a sustained release over 24 h, resulting in a final release of 30% of the loaded peptide

The charge of our particles, as determined by zeta potential and electrophoretic mobility, can be used to facilitate electrostatic loading of oppositely charged therapeutics, thereby increasing their loading efficiency beyond those obtained with simple passive loading (43,44). Previous work shows that unmodified sulfated poly(NIPAm) nanoparticles exhibit zeta potentials of approximately −15 mV, indicating that they are colloidally stable in an aqueous environment (43). The addition of a second negatively charged co-monomer to our particles reduced their zeta potential to approximately −35 mV. The addition of the cationic SILY peptide served to reduce the magnitude of the zeta potential and electrophoretic mobility compared to unmodified particles, though increasing the amount of SILY on the surface did not result in a further neutralization of the zeta potential. Increasing the temperature above the VPTT yielded no change in zeta potential, but resulted in an increase in electrophoretic mobility. This finding is promising as it indicates that the fully modified 100% NP-SILY particles should remain stable in an aqueous environment, while their highly negative charge allows for the electrostatic loading of positively charged therapeutics.

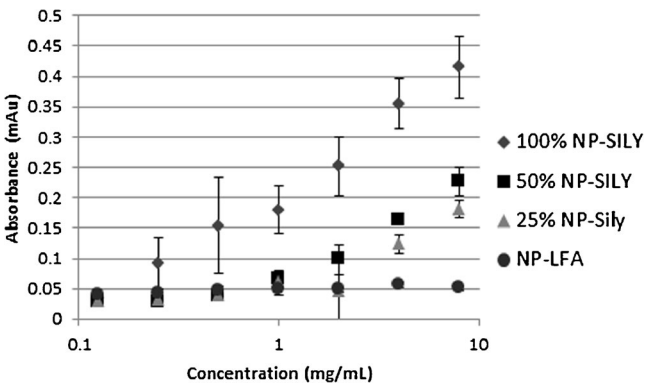

Fig. 4. A collagen binding assay demonstrated the modified particles' ability to bind to a collagen I-coated surface. Particle binding increased with an increase in conjugated SILY, while LFA-modified particles showed a complete inability to bind to the collagen plate

The electrostatic attraction between the sulfated nanoparticles and the SILY peptide raises the possibility that the SILY was simply electrostatically associated with the particle rather than covalently crosslinked. These weaker electrostatic associations would cause complications in nanoparticle targeting, as the SILY would be prone to disassociating from the nanoparticle in highly charged environments, such as those found within the body. Additionally, SILY peptides that are crosslinked via their terminal cysteine would have greater conformational freedom than those electrostatically associated with the particle surface. This would allow them to present the proper collagen-binding sites once suspended in an aqueous solution, and allow for competitive binding of the SILY to the exposed collagen while the nanoparticles would provide steric hindrance and prevent platelets from accessing any additional binding sites on the collagen (46,54). We found that while there is some electrostatic association between the particle and the SILY, a majority of the peptide is successfully covalently crosslinked to the particle using BMPH (Table II), resulting in a permanent stable attachment of the SILY peptide

The retention of their anionic charge and thermosensitive properties allows the modified nanoparticles to load and release the therapeutic peptide KAFAK, with a final loading efficiency of 32%, and a burst release of over 70% of the final amount of KAFAK released occurring within the first 12 h. This is slightly lower than the loading efficiencies reported by other sulfated poly(NIPAM) nanoparticles (29,43) and can most likely be attributed partial charge neutralization by the attached SILY as well as the surface-bound SILY hindering diffusion of the KAFAK into the particle's core. Decreased core loading could also explain the relatively rapid KAFAK release, as a large portion of the peptide would be near the surface of the particle allowing for rapid diffusion into the surrounding environment. Additionally the attached SILY, combined with the electrostatic attraction between the KAFAK and the particle, could hinder the release of any KAFAK that was successfully loaded into the core, resulting in the incomplete peptide release that was observed with these particles. Work has been done, in our lab and others, on the synthesis of degradable poly(NIPAM) nanoparticles (55–60), and it is likely that the use of a similar system in these particles would result in a more complete peptide release profile over a longer time period.

Due to the fact that each nanoparticle group contained the same amount of $SILY_{biotin}$, we were able to compare the relative binding affinity of particles with different amounts of SILY while ignoring any shielding of the biotin groups that could be caused by the particles binding to the collagen surface; however, it is possible that the data reported represents a slight underestimation of the actual modified particles true binding affinity. With these binding assays, we found that unmodified particles and those modified with a similarly charged but non-collagen-binding peptide showed minimal binding to a BSA blocked collagen-coated plate. Conversely, the SILY-modified particles are able to specifically bind to collagen, with the more heavily modified particles exhibiting increased binding ability. These nanoparticles are expected to remain bound to the collagen layer under physiological conditions, as studies with peptide targeted therapeutics and nanoparticle systems have shown them to be able to remain bound for several days *in vivo*

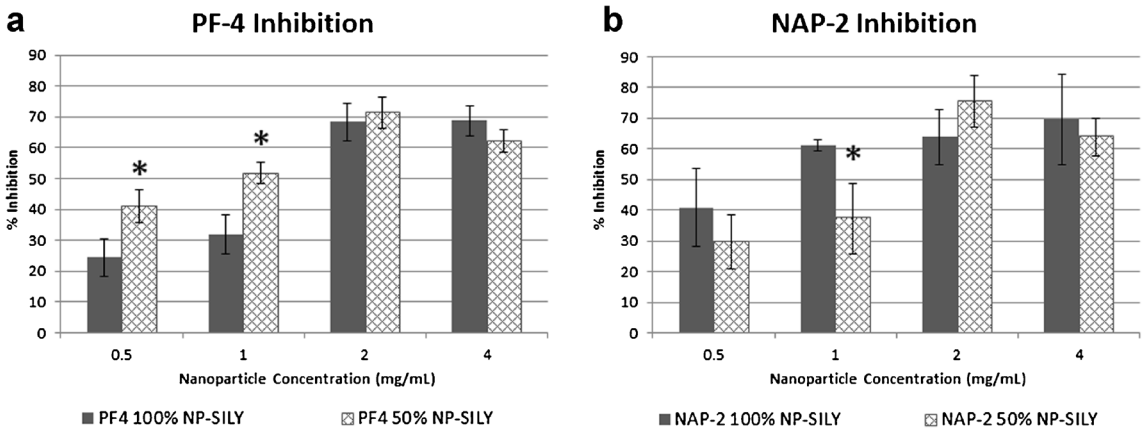

Fig. 5. Inhibition of collagen-induced platelet activation, as measured by the release of PF-4 (**a**) and NAP-2 (**b**). Inhibition increased with increasing NP-SILY concentration, with maximum inhibition occurring at a concentration of 2 mg/mL. *Asterisk* indicates significance from 100% modified particle

(46,61,62). Additionally, endocytic uptake of the loaded nanoparticles is expected to be minimal as they can be delivered directly to the damaged endothelium and allowed to bind to the collagenous layer that has been stripped of its native endothelial cells, allowing them to release their loaded peptide to the inflamed SMC.

Previous work in our lab has shown that a sulfated, collagen-binding therapeutic named DS-SILY is able to bind to collagen with a binding affinity of 24 nM and is able to remain bound to that surface for over 11 days (46). Additionally, DS-SILY demonstrated an ability to inhibit platelet activation by up to 60% for NAP-2, and 90% for PF-4 at concentrations of 10 μM when delivered to the damaged area through a porous angioplasty balloon. This was found to significantly reduce platelet activation-induced vasospasm and intimal hyperplasia in an ossabaw pig model when delivered to the damaged vessel via a porous catheter balloon (46,63). Given their size, our particles retain the ability to be delivered directly to the damaged endothelium in a similar manner and at concentrations up to 8 mg/mL. Once delivered *in vivo*, they would undergo hydrophobic collapse, triggering the controlled release of the loaded KAFAK allowing for the inhibition of local inflammation while simultaneously preventing platelet activation.

Our sulfated collagen-binding nanoparticles were able to successfully inhibit platelet activation, showing 30–40% inhibition of NAP-2 and PF-4 at concentrations of 0.5 mg/mL, and up to 70% inhibition at concentrations above 2 mg/mL. Interestingly, we observed higher inhibition of PF4 on the 50% modified particles at low concentrations, which disappeared as particle concentrations increased above 1 mg/mL. PF4 is known to bind to sulfated compounds, such as heparin, thereby reducing the concentration of free PF4 in solution (64,65). It is likely that a similar mechanism is occurring during the platelet inhibition studies, with the less modified particles having more of the charged nanoparticle surface available for association with the PF4. This would decrease free PF4 concentrations, resulting in an increase in platelet inhibition as reported by the PF4 ELISA. Our results demonstrate the particles' effectiveness at inhibiting collagen-mediated platelet activation, while the retention of their temperature sensitivity and charge characteristics allows them to load and release water-soluble therapeutics, such as therapeutic peptides.

CONCLUSION

We have developed a collagen-binding poly(NIPAm-MBA-AMPS-AAc) nanoparticle that is able to bind to a collagen coated plate, resulting in a decrease in collagen-mediated platelet activation by over 60% at nanoparticle concentrations above 0.5 mg/mL. In addition, the particles retained their temperature sensitivity exhibiting between a 9.3 to 13.2% decrease in particle size following hydrophobic collapse above their VPTT. Zeta potential and electrophoretic mobility measurements showed that the particles had a strong anionic charge, which can be used to electrostatically load charged therapeutics into the particle's core. Once exposed to physiological temperatures, the particles undergo a hydrophobic collapse, entrapping their loaded therapeutic and releasing it over 24 h. These properties mean that these particles are a viable dual therapy platform that can prevent collagen-mediated platelet activation following balloon angioplasty, while simultaneously delivering therapeutics directly to the injured vessel. Future work will focus on characterizing the particles' biocompatibility as well as their ability to bind to collagen under flow and in an *in vitro* cell culture system and potential for site-specific delivery via a porous angioplasty balloon. Additional *in vivo* studies will need to be conducted to further explore the translatability of these nanoparticles as a dual therapy system for the prevention of platelet activation and release of anti-inflammatory peptides.

REFERENCES

1. Cimminiello C, Borghi C, Kownator S, Wautrecht JC, Carvounis CP, Kranendonk SE, *et al.* Prevalence of peripheral arterial disease in patients at non-high cardiovascular risk. Rationale and design of the PANDORA study. BMC Cardiovasc Disord. 2010;10:35.

2. Criqui MH, Fronek A, Barrett-Connor E, Klauber MR, Gabriel S, Goodman D. The prevalence of peripheral arterial disease in a defined population. Circulation. 1985;71:510–5.
3. Hirsch AT, Criqui MH, Treat-Jacobson D, Regensteiner JG, Creager MA, *et al*. Peripheral arterial disease detection, awareness, and treatment in primary care. JAMA. 2001;286:1317–24.
4. Selvin E, Erlinger TP. Prevalence of and risk factors for peripheral arterial disease in the United States. Circulation. 2004;110:738–43.
5. Curt Diehm SL, Harald D, David P, von Stritzky B, Gerhart T, Haberl RL, *et al*. Association of low ankle brachial index with high mortality in primary care. Eur Heart J. 2006;27:1743–9.
6. Cacoub P, Cambou J-P, Leger P, Kownator S, Luizy F, Belliard J-P, *et al*. Prevalence of peripheral arterial disease in high-risk patients using ankle-brachial index in general practice: a cross-sectional study. Int J Clin Pract. 2009;63(1):63–70.
7. Aronow WS, Ahmed MI, Ekundayo OJ, Allman RM, Ahmed A. A propensity-matched study of the association of peripheral arterial disease with cardiovascular outcomes in community-dwelling older adults. Am J Cardiol. 2009;103(1):130–5.
8. Dalmia S, Pathak R, Callum K. Five-year duplex follow up of femoropopliteal percutaneous transluminal angioplasty. Indian J Surg. 2005;67:127–30.
9. Steele PM, Chesebro JH, Stanson AW, Holmes Jr DR, Dewanjee MK, Badimon L, *et al*. Balloon angioplasty. Natural history of the pathophysiological response to injury in a pig model. Circ Res. 1985;57(1):105–12.
10. Roberts DEAM, Bose R. Mechanism of collagen activation in human platelets. J Biol Chem. 2004;279:19421–30.
11. Farndale RW. Collagen-induced platelet activation. Blood Cells Mol Dis. 2006;36:162–5.
12. Amento EP, Ehsani N, Palmer H, Libby P. Cytokines and growth factors positively and negatively regulate interstitial collagen gene expression in human vascular smooth muscle cells. Atheroscler Thromb. 1991;11:1223–30.
13. Hanke H, Strohschneider T, Oberhoff M, Betz E, Karsch KR. Time course of smooth muscle cell proliferation in the intima and media of arteries following experimental angioplasty. Circ Res. 1990;67:651–9.
14. Karas SPMBG, Santoian EC, Robinson KA, Anderberg KA. Coronary intimal proliferation after balloon injury and stenting in swine: an animal model of restenosis. J Am Coll Cardiol. 1992;20:467–74.
15. MacLeod DC, Strauss BH, de Jong M, Escaned J, Umans VA. Proliferation and extracellular matrix synthesis of smooth muscle cells cultured from human coronary atherosclerotic and restenotic lesions. J Am Coll Cardiol. 1994;23:59–65.
16. Jessica Perez RAT, Darley-Usmar VM, Petra R, Cismowski MJ, Weber DS, Lucchesi PA. PYK2 signaling is required for PDGF-dependent vascular smooth muscle cell proliferation. Am J Physiol Cell Physiol. 2011;301:C242–51.
17. Loppnow H, Bil R, Hirt S, Schönbeck U, Herzberg M, Werdan K, *et al*. Platelet-derived interleukin-1 induces cytokine production, but not proliferation of human vascular smooth muscle cells. Blood. 1998;91:134–91.
18. Daemen J, Wenaweser P, Tsuchida K, Abrecht L, Vaina S, Morger C, *et al*. Early and late coronary stent thrombosis of sirolimus-eluting and paclitaxel-eluting stents in routine clinical practice: data from a large two-institutional cohort study. Lancet. 2007;24(9562):667–78.
19. Arturo Garcia-Touchard SEB, Toner JL, Cromack K, Robert S. Schwartz Zotarolimus-eluting stents reduce experimental coronary artery neointimal hyperplasia after 4 weeks. Eur Heart J. 2006;27(8):988–93.
20. Christian M, Matter IR, Jaschko A, Greutert H, Kurz D, Wnendt S, *et al*. Effects of tacrolimus or sirolimus on proliferation of vascular smooth muscle and endothelial cells. J Cardiovasc Pharm. 2006;48(6):286–92.
21. Joner M, Finn AV, Farb A, Kolodgie FD, Ladich E, Kutys R, *et al*. Pathology of drug-eluting stents in humans: delayed healing and late thrombotic risk. J Am Coll Cardiol. 2006;48(1):193–202.
22. Joner M, Virmani R, Kolodgie FD, Gold HK, Xu X, Skorija K, *et al*. Endothelial cell recovery between comparator polymer-based drug-eluting stents. J Am Coll Cardiol. 2008;52(5):333–42.
23. Krajcer ZMHH. Update on endovascular treatment of peripheral vascular disease. Tex Heart Inst J. 2000;27:369–85.
24. Mongiardo A, Curcio A, Spaccarotella C, Parise S, Indolfi C. Molecular mechanisms of restenosis after percutaneous peripheral angioplasty and approach to endovascular therapy. Curr Drug Targets Cardiovasc Haematol Disord. 2004;4:275–87.
25. Schillinger M, Sabeti S, Loewe C, Dick P, Amighi J, Mlekusch W, *et al*. Balloon angioplasty versus implantation of nitinol stents in the superficial femoral artery. N Engl J Med. 2006;354:1879–88.
26. Galperin ATJL, Ratner BD. Degradable, thermo-sensitive poly(N-isopropyl acrylamide)-based scaffolds with controlled porosity for tissue engineering applications. Biomacromolecules. 2010;11:2583–92.
27. Overstreet DJ, Huynh R, Jarbo K, McLemore RY, Vernon BL. In situ forming, resorbable graft copolymer hydrogels providing controlled drug release. J Biomed Mater Res A. 2013;101A:1437–46.
28. Overstreet DJRYM, Doan BD, Farag A, Vernon BL. Temperature-responsive graft copolymer hydrogels for controlled swelling and drug delivery. Soft Mater. 2013;11(3):294–304.
29. Saikia AK, Saroj A, Mandal UK. Preparation and controlled drug release characteristics of thermoresponsive PEG/Poly (NIPAMco-AMPS) hydrogels. Int J Polym Mater Polym Biomater. 2012;62(1):39–44.
30. Jones CD, Lyon LA. Dependence of shell thickness on core compression in acrylic acid modified poly(N-isopropylacrylamide) core/shell microgels. Langmuir. 2003;19(11):4544–7.
31. Schmaljohann D. Thermo- and pH-responsive polymers in drug delivery. Adv Drug Deliv Rev. 2006;58(15):1655–70.
32. Elaissari A. Thermally sensitive colloidal particles: from preparation to biomedical applications. Smart Colloid Mater. 2006;133(9):9–14.
33. LA Lyon MZ, Singh N, Sorrell CD, John AS. Thermoresponsive microgel-based materials. Chem Soc Rev. 2009;38(4):865–74.
34. Lau AK, Leichtweis SB, Hume P, Mashima R, Hou JY, Chaufour X, *et al*. Probucol promotes functional reendothelialization in balloon-injured rabbit aortas. Circulation. 2003;107:2031–6.
35. Yallapu MM, Vasir JK, Jain TK, Vijayaraghavalu S, Labhasetwar V. Synthesis, characterization and antiproliferative activity of rapamycin-loaded poly(N-isopropylacrylamide) based nanogels in vascular smooth muscle cells. J Biomed Nanotechnol. 2008;4:16–24.
36. Gan DJ, Lyon LA. Tunable swelling kinetics in core-shell hydrogel nanoparticles. J Am Chem Soc. 2001;123:7511–7.
37. Liu Y, Li Z, Liang D. Behaviors of liposomes in a thermo-responsive poly(N-isopropylacrylamide) hydrogel. Soft Matter. 2012;8:4517–23.
38. Kratza K, Hellwegb T, Eimera W. Influence of charge density on the swelling of colloidal poly(N-isopropylacrylamide-co-acrylic acid) microgels. Colloids Surf A Physiochem Eng Asp. 2000;170(2):137–49.
39. Meng Z, Cho JK, Debord S, Breedveld V, Lyon LA. Crystallization behavior of soft, attractive microgels. J Phys Chem B. 2007;111(25):6992–7.
40. Blackburn WH, Lyon LA. Size-controlled synthesis of monodisperse core/shell nanogels. Colloid Polym Sci. 2008;286(5):563–9.
41. Blackburn WH, Dickerson EB, Smith MH, McDonald JF, Lyon LA. Peptide-functionalized nanogels for targeted siRNA delivery. Bioconj Chem. 2009;20(5):960–8.
42. Weissleder RKK, Sun EY, Shtatland T, Josephson L. Cell-specific targeting of nanoparticles by multivalent attachment of small molecules. Nat Biotechnol. 2005;23(11):1418–23.
43. Bartlett R, Medow M, Panitch A, Seal B. Hemocompatible poly(NIPAm-MBA-AMPS) colloidal nanoparticles as carriers of anti-inflammatory cell penetrating peptides. Biomacromolecules. 2012;13(4):1204–11.
44. Bartlett R, Sharma S, Panitch A. Cell-penetrating peptides released from thermosensitive nanoparticles suppress pro-inflammatory cytokine response by specifically targeting inflamed cartilage explants. Nanomedicine: NBM. 2013;9:419–27.
45. John Paderi AP. Design of a synthetic collagen-binding peptidoglycan that modulates collagen fibrillogenesis. Biomacromolecules. 2008;9:2562–6.

46. Paderi JE, Stuart K, Sturek M, Park K, Panitch A. The inhibition of platelet adhesion and activation on collagen during balloon angioplasty by collagen-binding peptidoglycans. Biomaterials. 2011;32:2516–23.
47. Brugnano J, Chan BK, Seal BL, Panitch A. Cell-penetrating peptides can confer biological function: regulation of inflammatory cytokines in human monocytes by MK2 inhibitor peptides. J Control Release. 2011;155(2):128–33.
48. Liu R, Fraylich M, Saunders BR. Thermoresponsive copolymers: from fundamental studies to applications. Colloid Polym Sci. 2009;287(6):627–43.
49. White B, Banerjee S, Stephen O'B, Turro NJ, Herman IP. Zeta-potential measurements of surfactant-wrapped individual single-walled carbon nanotubes. J Phys Chem C. 2007;111:13684–90.
50. Karen Kaplan JO. Plasma levels of 9-thromboglobulin and platelet factor 4 as indices of platelet activation in vivo. Blood. 1981;57(2):199–202.
51. Peter M, Newman BHC. Heparin-induced thrombocytopenia: new evidence for the dynamic binding of purified anti-PF4–heparin antibodies to platelets and the resultant platelet activation. Blood. 2000;96(1):182–7.
52. Weng Y, Ding Y, Zhang G. Microcalorimetric investigation on the lower critical solution temperature behavior of N-isopropycrylamide-co-acrylic acid copolymer in aqueous solution. J Phys Chem B. 2006;110(24):11813–7.
53. Anna Burmistrova MR, Eisele M, Uzum C, von Klitzing R. The effect of co-monomer content on the swelling/shrinking and mechanical behaviour of individually adsorbed PNIPAM microgel particles. Polymers. 2011;3:1575–90.
54. Kang TM, Ca AH. A synthetic peptide derived from the sequence of a type I collagen receptor inhibits type I collagen-mediated platelet aggregation. J Clin Invest. 1997;100(8):2079–84.
55. Bartlett RL, Panitch A. Thermosensitive nanoparticles with pH-triggered degradation and release of anti-inflammatory cell-penetrating peptides. Biomacromolecules. 2012;13(8):2578–84.
56. Cui Z, Lee BH, Pauken C, Vernon BL. Degradation, cytotoxicity, and biocompatibility of NIPAAm-based thermosensitive, injectable, and bioresorbable polymer hydrogels. J Biomed Mater Res A. 2011;98A(2):159–66.
57. Mizuntani M, Satoh K, Kamigaito M. Degradable poly(N-isopropylacrylamide) with tunable thermosensitivity by simultaneous chain- and step-growth radical polymerization. Macromolecules. 2011;44:2382–6.
58. Poh S, Lin JB, Panitch A. Release of anti-inflammatory peptides from thermosensitive nanoparticles with degradable cross-links suppresses pro-inflammatory cytokine production. Biomacromolecules. 2015;16(4):1191–200.
59. Zhao CXG, He P, Xiao C, Zhuang X, Chen X. Facile synthesis of thermo- and pH-responsive biodegradable microgels. Colloid Polym Sci. 2011;289:447–51.
60. Yoshida ATA, Kokufuta E, Okano T. Newly designed hydrogel with both sensitive thermoresponse and biodegradability. J Polym Sci A Polym Chem. 2002;41:779–87.
61. McAteer MA, Schneider JE, Ali ZA, Warrick N, Bursill CA, Muhlen C v z, *et al*. Magnetic resonance imaging of endothelial adhesion molecules in mouse atherosclerosis using dual-targeted microparticles of iron oxide. Arterioscler Thromb Vasc Biol. 2008;28:77–83.
62. Park K, Hong YH, Moon HJ, Lee BH, Kwon IC, Rhee K, *et al*. A new atherosclerotic lesion probe based on hydrophobically modified chitosan nanoparticles functionalized by the atherosclerotic plaque targeted peptides. J Control Release. 2008;128:217–23.
63. Scott RS, Paderi JE, Sturek M, Panitch A. Decorin mimic inhibits vascular smooth muscle proliferation and migration. PLOS One. 2013;8(11).
64. Cardin AD, HJRW. Molecular modeling of protein-glycosaminoglycan interactions. Atheroscler Thromb Vasc Biol. 1988;9(1):21–32.
65. John G, Kelton JWS, Warkentin TE, Hayward CPM, Denomme GA, Horsewood P. Immunoglobulin G from patients with heparin-induced thrombocytopenia binds to a complex of heparin and platelet factor 4. Blood. 1994;83(11):3232–9.